Journal of the Korean Chemical Society
2012, *Vol. 56, No. 1*
Printed in the Republic of Korea
http://dx.doi.org/10.5012/jkcs.2012.56.1.034

Carbon Nanotubes Doped with Nitrogen, Pyridine-like Nitrogen Defects, and Transition Metal Atoms

Michael R. Mananghaya*
Physics Department, Mapua Institute of Technology, Philippines.
**E-mail: mike_mananghaya@yahoo.com*
(Received October 10, 2011; Accepted December 12, 2011)

ABSTRACT. Dopants and defects can be introduced as well as the intercalation of metals into single wall carbon nanotubes (SWCNTs) to modify their electronic and magnetic properties, thus significantly widening their application areas. Through spinpolarized density functional theory (DFT) calculations, we have systemically studied the following: (i) (10,0) and (5,5) SWCNT doped with nitrogen (CN_xNT), (ii) (10,0) and (5,5) SWCNT with pyridine-like defects (3NV-CN_xNT), and (iii) chemical functionalization of (10,0) and (5,5) 3NV-CN_xNT with 12 different transition metals (TMs) (Sc, Ti, V, Cr, Mn, Fe, Co, Ni, Cu, Zn, Pd, and Pt). Attention was done in searching for the most stable configurations, deformation, calculating the formation energies, and exploring the effects of the doping concentration of nitrogen and pyridine-like nitrogenated defects on the electronic properties of the nanotubes. Also, calculating the corresponding binding energies and effects of chemical functionalization of TMs on the electronic and magnetic properties of the nanotubes has been made. We found out that the electronic properties of SWCNT can be effectively modified in various ways, which are strongly dependent not only on the concentration of the adsorbed nitrogen but also to the configuration of the adsorbed nitrogen impurities, the pyridine-like nitrogenated defects, and the TMs absorbed; due to the strong interaction between the d orbitals of TMs and the p orbitals of N atoms, the binding strengths of TMs with the two 3NV-CN_xNT are significantly enhanced when compared to the pure SWCNTs.

Key words: Binding energy, Density functional theory, Nitrogenated single-walled carbon nanotubes, Transition metals

INTRODUCTION

Single-walled carbon nanotubes (SWCNTs) can be metallic or semi-conducting, depending greatly on their tubular diameter and chirality. Thus it is difficult to synthesize SWCNTs with uniform chirality and electronic properties. To overcome this difficulty, dopants and defects can be introduced to alter the electronic properties of SWCNTs. Recently; chemical functionalization of carbon nanotubes (CNTs) with various groups has attracted considerable interest as an efficient way to modify their properties.[1-6]

B and/or N atoms are also good choice of dopants because they have roughly the same atomic radius as C atoms, and possess one electron less/more than C respectively. Nitrogen doping is particularly attractive because the extra electrons from the nitrogen dopants are expected to make semiconducting nanotubes metallic. The N-doped CNTs (CN_xNTs) has been synthesized in several groups.[7-12] Various approaches have been made to incorporate nitrogen atoms into carbon nanotubes, including magnetron sputtering,[13] pyrolysis of nitrogen-rich organic chemicals,[14] and arc-discharge in nitrogen atmosphere.[15] However, most of the syntheses yield nitrogen-doped multiwalled carbon nanotubes (N-MWCNT) with bamboo-shaped morphology. Recently, Villalpando-Paez *et al*.[16] reported the synthesis of nitrogen-doped SWNT bundles via an aerosol-assisted chemical vapor deposition (CVD) method, but the doping concentration is unknown. It has been suggested that the nitrogen dopants are substituted into the carbon network with and without vacancy formation. Electron energy loss spectroscopy and X-ray photoelectron spectroscopy measurements indicated the coexistence of pyridine-like and porphyrine-like structures.[9,10] For the pyridine-like, nitrogen substitution accompanied with vacancy (labeled as 3NV) is formed in the sidewall of SWCNT, the electronic,[17] field emission,[18] and electrical transport properties[19] have been systemically investigated. The presence of 3NV defects in CNT, suggests that the reactivity might be greatly enhanced compared with the pure CNT, thus becoming a recently hot topic.[16,20-28] By introducing new levels close to the Fermi level, doping with nitrogen can change the sensibility of CNT to different kinds of molecules, for example the CN_xNTs can be used as gas sensors of toxic species.[16,20] Moreover, the capability of Li storage in the CN_xNT is significantly increased for battery applications.[21]

3*d* Transition metals (TMs) are frequently used to synthesize SWCNTs and can mix with the nanotubes to affect

their electronic and magnetic properties. Aside from modification of the electronic and magnetic properties of CNTs through nitrogen doping and 3NV defects, it can also typically be effectively modified through chemical decoration of TMs,[29-31] which greatly expands the potential application areas of CNTs, such as improving the sensitivities of chemical sensors, providing higher reactive sites for hydrogen gas storages, and developing spintronic devices or catalysts. For example, the CN_xNT is a promising candidate as a support material to immobilize various TM nanoparticles, which have been found to exhibit good catalytic property.[24-28,32-37] Furthermore, Shao *et al*.[25] have demonstrated that the Pt/CN_xNT is an excellent material for proton exchange membrane fuel cell. Additionally, Su *et al*.[26] have shown that the Pt/ CN_xNT nanocatalyst exhibits good catalytic activities toward methanol oxidation and oxygen reduction reactions.

Compared with these experimental advances in the interactions between TMs and CN_xNTs, to our knowledge, there are only a few theoretical studies on this issue:[38-42] (1) through density functional theory (DFT) calculations,[38,39] Yang and Li have independently reported that the binding energy of Ni or Pt interacting with the CNT is significantly improved in the presence of the 3NV defect in the CNT. (2) Feng *et al*.[40] theoretically studied adsorptions of different TMs on three kinds of CN_xNT on aiming to evaluate the catalytic performance of Pt/CN_xNT, they have further investigated its interaction with several common species involved in methanol oxidation, including CH_3OH, HCHO, and HCOOH. (3) Titov *et al*.[41,43] have explored the stability of Fe-adsorbed CN_xNTs with porphyrine-like defect through the bent-cluster model.

However, the following issues still need to be addressed: (1) effects of nitrogen and pyridine-like nitrogen doping on CNTs atomic deformation, molecular orbital, electronic structures and properties; (2) the bonding nature between different TMs and the CNT with 3NV defect (3NV-CN_xNT); (3) the effects of various TMs adsorptions on the magnetic and electronic properties of 3NV-CN_xNT; Thus, in the present work, nitrogen doping at various concentrations, pyridine-like doping, and the chemical functionalization of 12 different TMs (Sc, Ti, V, Cr, Mn, Fe, Co, Ni, Cu, Zn, Pd, and Pt) on a (10,0) and (5,5) CNT with 3NV defect has been systematically studied through spin-polarized DFT calculations. Particular attention has been paid to locating the most stable configurations, deformation, calculating corresponding formation energies, and exploring the effects of the doping concentration of nitrogen and pyridine-like defects. Also, calculating the corresponding binding energies and effects of TMs adsorptions on the electronic and magnetic properties of nanotube, which is useful for further studying the adsorptions of TM clusters on CN_xNTs.

Study of the doping of N impurities and interactions of TMs with nanotubes is important to understand their potential applications, including nanowires, high strength composites, metal coated structures, nanoelectronic devices, spintronic devices, etc. Specifically, the creation of new energy levels in the band gap with associated electronic states through doping of impurities is an important step to make electronic devices. Further, the interaction of magnetic atoms with nanotubes could lead to half metallic systems important because of their unique magneto-transport properties that are of interest for spintronic devices as well as nanomagnets and it is a necessity to know which elements can best be bonded with nanotubes and how the magnetic properties are affected.

METHODOLOGY

The electronic properties of nitrogenated SWCNTs were studied using first-principles density functional theory (DFT), $Dmol^3$ code, available from Accelrys.[44] Each electronic wave function is expanded in a localized atom-centered basis set with each basis function defined numerically on a dense radial grid. For supercell geometries, spin-unrestricted calculations were carried out with a double numeric polarized (DNP) basis set available and the atomic cutoff set at 4.6Å, along with gradient-corrected Perdew-Burke-Ernzerhof (PBE) functional.[45] Scalar relativistic effects[46] were included via a local pseudopotential for all-electron calculations. Five and ten Monkhorst-Pack *k*-points[47] were used for the Brillouin zone integration along the axes of (10,0) and (5,5) nanotubes, respectively. Geometry optimizations were performed with the Broyden-Fletcher-Goldfarb-Shanno (BFGS) algorithm with convergence criterion of 0.005Å on displacement, and 10^{-5} a.u. on the total energy and electron density. A hexagonal lattice was used to simulate the single-walled nanotubes, with a wall-to-wall distance of at least 10Å, sufficient to avoid in-plane interactions between nanotubes in adjacent unit cells. The Fermi levels of the spin-unrestricted band structures and density of states (DOS) of (10,0) and (5,0) nanotubes were reset at the 0 eV position. For $Dmol^3$ code, the molecular orbital of periodic systems was computed using only the Γ-point. The isodensity surfaces of highest occupied molecular orbital (HOMO) were fixed at 0.02 e/$a.u.^3$.

Calculations were performed with supercells of zigzag (10,0) (see *Fig*. 1a-d) and armchair (5,5) SWNTs (see *Fig*.

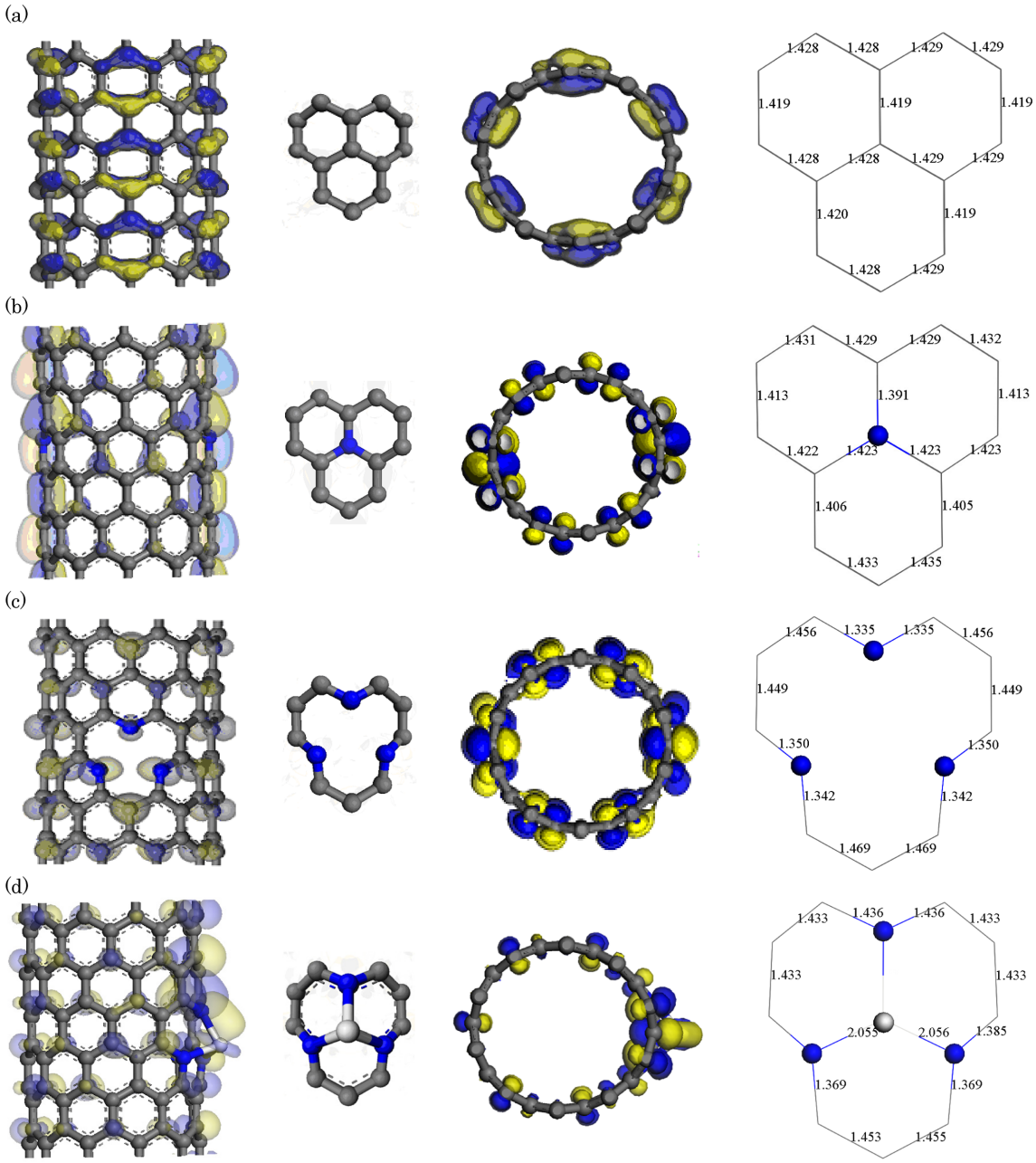

***Fig.* 1.** Geometrically optimized structures (a), highest occupied molecular orbital (HOMO) and bond lengths (in Å) of a pure zigzag (10,0) nanotube, (b) direct substitution of two nitrogen atoms into the carbon framework. Here the two N substitution atoms in $C_{118}N_2$ are in the opposite positions, (c) N substitution into the carbon framework with the formation of pyridine-like vacancy: pyridine-like doping ($C_{112}N_6$) Two vacancies formed in opposite positions, (d) Adsorption configuration of the transition metal on a nanotube with pyridinelike defect. Grey ball denotes C atom, blue ball denotes N atom, and white denotes TM (Sc). A fragment of the supercell was taken out to elucidate the bong lengths at the vicinity of the N/TM impurities.

2a-d). The supercell length of the zigzag (120 atoms/cell) and armchair (100 atoms/cell) nanotubes are a=12.78Å and a=12.30Å respectively. Three types of modified nanotubes were considered: (i) Direct substitution of nitrogen dopants into the carbon framework without a formation of vacancy at 1.67% (*Fig.* 1b) for (10,0) and at 2.0% (*Fig.* 2b) for (5,5). Doping density varies from 0.83-2.0%. (ii) Substitution of nitrogen dopants with vacancy formation, by removing a central C atom among three hexagons and replacing the three surrounding C atoms with 3 N atoms (3NV-CN_xNT) at 5.08% (*Fig.* 1c) for (10,0) and at 6.12% (*Fig.* 2c) for (5,5). Doping density varies from 2.52-6.12%.

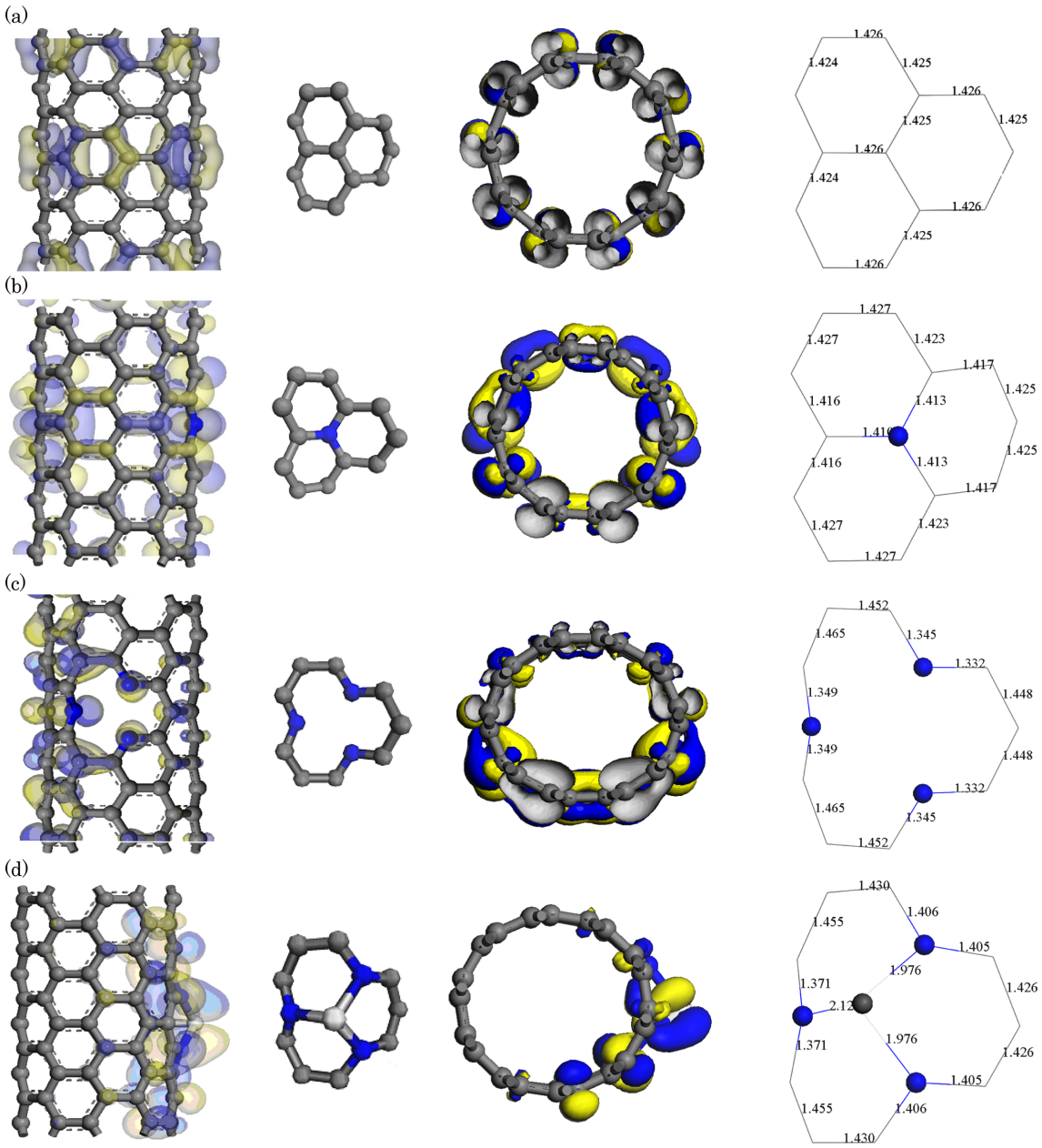

***Fig.* 2.** Geometrically optimized structures (a), highest occupied molecular orbital (HOMO) and bond lengths (in Å) of a pure armchair (5,5) nanotube, (b) direct substitution of two nitrogen atoms into the carbon framework. Here the two N substitution atoms in $C_{98}N_2$ are in the opposite positions, (c) N substitution into the carbon framework with the formation of pyridine-like vacancy ($C_{92}N_6$). Two vacancies formed in opposite positions, (d) Adsorption configuration of the transition metal on a nanotube with pyridinelike defect. Grey ball is C atom, blue ball is N atom, and white is TM (Sc). A fragment of the supercell was taken out to elucidate the bong lengths at the vicinity of the N/TM impurities.

(iii) Chemical functionalization of 12 different TMs (Sc, Ti, V, Cr, Mn, Fe, Co, Ni, Cu, Zn, Pd and Pt) on 3NV-CN_xNT (see *Figs*. 1d and 2d).

Specifically, in the direct substitution of nitrogen dopants the impurities are on opposite sides of the tube. Although the interaction between the two impurities is weak, we will see that the resulting bands are not simply related to concentration of impurities, but also the way N are distributed in the unit cell. It is evident that in order to have a realistic description of doped CNTs a random distribution of impurities should be used. However we suppose an ideal situation in which impurities are distributed in a periodic cell can provide useful insights on the doping effects in a less computationally expensive way.

RESULTS AND DISCUSSIONS

Structural parameters

Figs. 1 and 2 show the relaxed geometries of (10,0) and (5,5) nanotubes respectively, along with the distribution of the highest-occupied molecular orbital (HOMO) of (10, 0) and (5,5) SWCNT. Pure (10,0) and (5,5) SWCNT with the diameter of 7.83 and 6.78Å respectively was chosen in the present work. Generally, it is noted that the cylindrically pristine nanotube is deformed to an ellipsoidal shape upon doping. A deformation factor (δ) is defined as the ratio of the major axis to the minor axis of the nanotubes. The δ values for the various types of nitrogenation are listed in *Table* 1, for pyridine-like doping, a (5,5) nanotube (δ1.3) suffers a larger deformation than a (10,0) nanotubes (δ1.1) due to the smaller diameter of (5,5) nanotube.

The bond lengths of the relaxed nanotubes in the vicinity of the nitrogen impurities are also displayed in *Fig*. 1 and 2. The C-N bond lengths of direct nitrogen substitution are determined to be ~1.39-1.42Å for the doped nanotubes both in *Fig*. 1b and *Fig*. 2b. Due to the missing central C atom, the C-N bond lengths of pyridine-like doping are determined to be ~1.33-1.35Å, depending on the orientation, as compared to ~1.42-1.43Å for the C-C bonds (see *Figs.* 1c and 2c). The relaxed structures of nitrogenated SWCNTs correlate well with experimental observations of compartmentalized and defective nitrogen-doped CNTs.[14,48] When an individual TM atom is adsorbed on the CN_xNT, we consider two kinds of initial configurations: (1) the TM is directly bound to the site of 3NV; (2) the TM is attached to the sites near 3NV. After full structural optimization, we find that the TM adsorptions on the defect sites (*Figs.* 1d and 2d) are the most stable because of their higher reactivity than other sites.[16,20,21,38-43] Accordingly, in *Table* 2, we list the structural parameters most stable configurations of TMs adsorbed on the two 3NV-CN_xNT (labeled as TM/3NV-CN_xNT). We find that these most stable configurations of TM/3NV-CN_xNT nanotubes are characterized as forming multiple TM-N bonds at the vacancy sites (*Fig*. 1d and 2d) due to the N participation. All the TMs are projecting from the sidewall of the two 3NV-CN_xNTs in various ways. Moreover, as shown in *Table* 2, the average TM-N distances (d_{TM-N}) of TM/CN_xNT nanotubes with 3NV defects range from 1.84 (Fe) to 2.25 (Pd) Å for (10,0) and from 1.82 (Co) to 2.26 (Pd) Å for (5,0). Thus it can be surmised that N and TM impurities in CNTs produce their own local strains and results in the respective deformation.

The effects of dissimilar nitrogenation on armchair and zigzag nanotubes are also reflected by the differences in the HOMO distribution. For instance, the HOMO of a nitrogen substituted (10,0) nanotube is polarized at two opposite nitrogen dopants, while this is not the case for a nitrogen substituted (5,5) nanotube (see *Fig*. 1b and 2b). Pyridine-like doping causes the HOMO of doped (5,5) nanotube to be more concentrated at one side of the ellip-

***Table* 1.** Calculated deformation (δ) of the (10,0) and (5,5) nitrogenated SWCNTs

	System	δ
(10,0)	Pure C_{120}	1.0
	Substitution, $C_{118}N_2$	1.1
	Pyridine-like, $C_{112}N_6$	1.1
	Sc/3NV-CN_xNT, $ScC_{116}N_3$	1.1
(5,5)	Pure C_{100}	1.0
	Substitution, $C_{98}N_2$	1.1
	Pyridine-like, $C_{92}N_6$	1.3
	Sc/3NV-CN_xNT, $ScC_{96}N_3$	1.1

***Table* 2.** Calculated average TM-N bond lengths (D_{TM-N}), binding energies (E_b) of various TMs adsorbed on (10,0) and (5,5) CNT with pyridine-like defect, the charge transferred (C) from TM to the (10,0) and (5,5) CNT with pyridine-like defect, and the net magnetic moment of the (10,0) and (5,5) CNT with pyridine-like defect functionalized with transition metals (μ_{total})

	System	D_{TM-N}(Å)	E_b (eV)	C (e)	μ_{total}
(10,0)	Sc	2.02	-7.58	0.70	0.00
	Ti	1.95	-7.04	0.56	0.97
	V	1.88	-6.06	0.46	0.02
	Cr	1.87	-4.40	0.53	1.85
	Mn	1.86	-4.58	0.26	0.00
	Fe	1.84	-5.66	0.29	0.00
	Co	1.88	-5.62	0.18	1.72
	Ni	1.85	-4.96	0.16	1.00
	Cu	1.93	-3.56	0.30	0.00
	Zn	1.94	-1.88	0.42	0.00
	Pd	2.25	-2.04	0.36	0.60
	Pt	2.15	-2.66	0.24	0.82
(5,5)	Sc	2.02	-7.31	0.70	0.00
	Ti	1.98	-6.74	0.55	1.39
	V	1.96	-6.41	0.42	2.54
	Cr	1.88	-4.29	0.55	2.01
	Mn	1.86	-4.35	0.26	0.00
	Fe	1.84	-5.61	0.28	0.00
	Co	1.82	-5.36	0.20	0.00
	Ni	1.86	-4.82	0.19	1.13
	Cu	1.92	-3.37	0.30	0.00
	Zn	1.91	-1.73	0.48	0.00
	Pd	2.26	-1.86	0.36	0.60
	Pt	2.08	-2.55	0.25	0.82

soidal ring (see *Figs.* 1c and 2c). The HOMO of the nanotube functionalized with a TM is polarized at the TM dopants for both (10,0) and (5,5) nanotubes (see *Figs*. 1d and 2d).

Formation Energies

We choose the (10,0) tube as a typical semi conducting tube for investigation and suggest that two nitrogen doped atoms might be very near to or far from each other, but which configuration is stable favorable completely depends on its formation energy. Stability can be assessed by calculating their formation energies (E_f) here the formation energy is defined as

$$E_f = E_{tot} - n_C\mu_C - n_N\mu_N \quad (1)$$

where E_{tot} is the total energy of the (10,0) and (5,5) CN_xNT, n_C, and n_N are the number of C and N atoms, respectively. μ_C is the chemical potential of C obtained from the corresponding pure CNT, and is the chemical potential of μ_N obtained from nitrogen in gas phase. There are six configurations in which adjacent nitrogen substituted (NS) atoms are near and lie in the same hexagon, as shown in *Fig*. 3, which are denoted by NS1 to NS6, respectively. For the other case, the typical configuration that the two nitrogen atoms are apart is chosen, denoted by NS7 as shown in *Fig.* 3. The formation energies of the nitrogenated SWCNTs were given in *Table* 3. It is clear from the table that NS1 and NS2 atoms shown in *Figs*. 3a and 3b are energetically unfavorable and that the most stable is NS5, shown in *Fig.* 3e because its configuration is symmetric along the tube axis. The stable configurations for CN_xNT are sensitive to symmetry. NS6 and NS7 have the same formation energies. Interestingly, if we compare the band structures of two nitrogen doped atoms near to or far from each other (NS5 and NS7) we see from *Fig.* 3h and 3i that NS6 is still a semiconductor while NS7 has been transformed to metallic. This motivates us to choose NS7 as a model for investigating the effects of nitrogen substitution for (10,0) nanotubes. Particularly the model is so chosen to represent the effects of nitrogen doping on CNTs atomic deformation, molecular orbital, electronic structures and properties.

***Table* 3.** Formation energies of (10,0) and (5,5) N-substituted (NS) and pyridine-like doped SWNTs

	System	E_f (eV)
(10,0)	NS1	3.12
	NS2	2.75
	NS3	2.30
	NS4	2.30
	NS5	1.84
	NS6	2.12
	NS7	2.15
	Substitution, $C_{119}N_1$	1.05
	Substitution, $C_{118}N_2$	2.15
	Pyridine-like, $C_{116}N_3$	3.35
	Pyridine-like, $C_{112}N_6$	6.71
(5,5)	Substitution, $C_{99}N_1$	1.09
	Substitution, $C_{98}N_2$	2.15
	Pyridine-like, $C_{96}N_3$	3.11
	Pyridine-like, $C_{92}N_6$	6.10

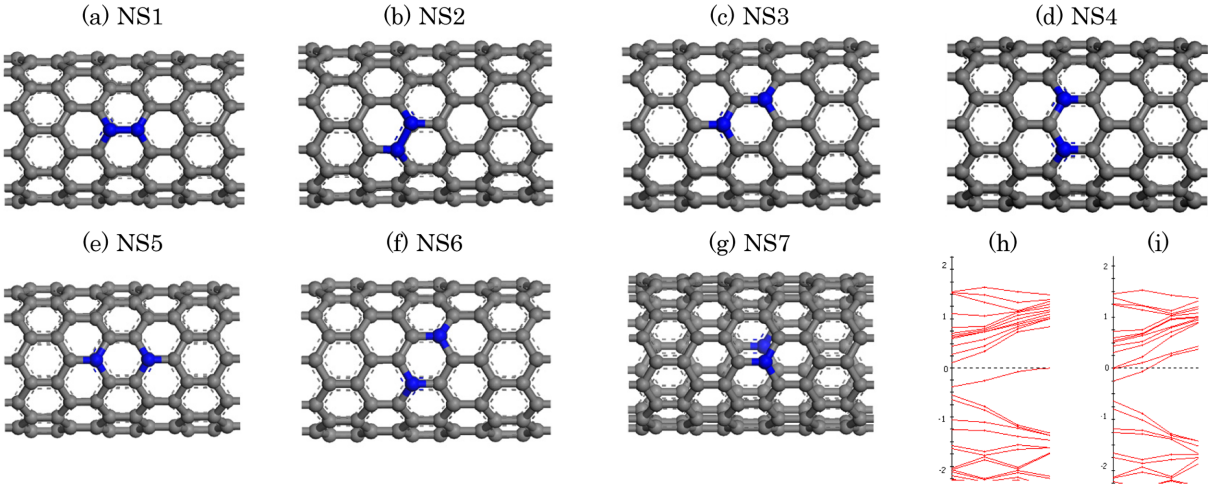

***Fig.* 3.** Geometrically optimized structures of the configurations for (10,0) tubes containing two substitutional nitrogen atoms per five tube units denoted by (a) NS1-(g) NS7, respectively and the bandstructures of (h) NS5 and (i) NS7 configurations. Substitutional nitrogen atoms are denoted by blue balls, Grey ball is C atom.

The energy cost to sp^2-substitute a C atom with an N atom in (10,0) and (5,5) nanotubes are 1.05 and 1.09 eV respectively. On the other hand, it costs 3.35 and 3.11 eV to form pyridine-like doping in (10,0) and (5,5) nanotubes respectively. The synthesis of N-doped carbon nanotubes is usually carried out at 700-900 °C using nitrogen-rich precursors for CVD processes.[14,49,50] Spectroscopic studies and peak analysis revealed that C-N bonding of N-doped carbon nanotubes involved sp^2, sp^3-typed and intercalated N_2 as well, which might be attributed to sp^2-substitution of C atom with an N atom, pyridine-like doping and molecular N_2 respectively. The relatively high synthesis temperature and use of catalysts might provide sufficient energies to form pyridine-like defects in N-doped carbon nanotubes, though the formation energies of pyridine-like defects is higher than sp^2-substitution.

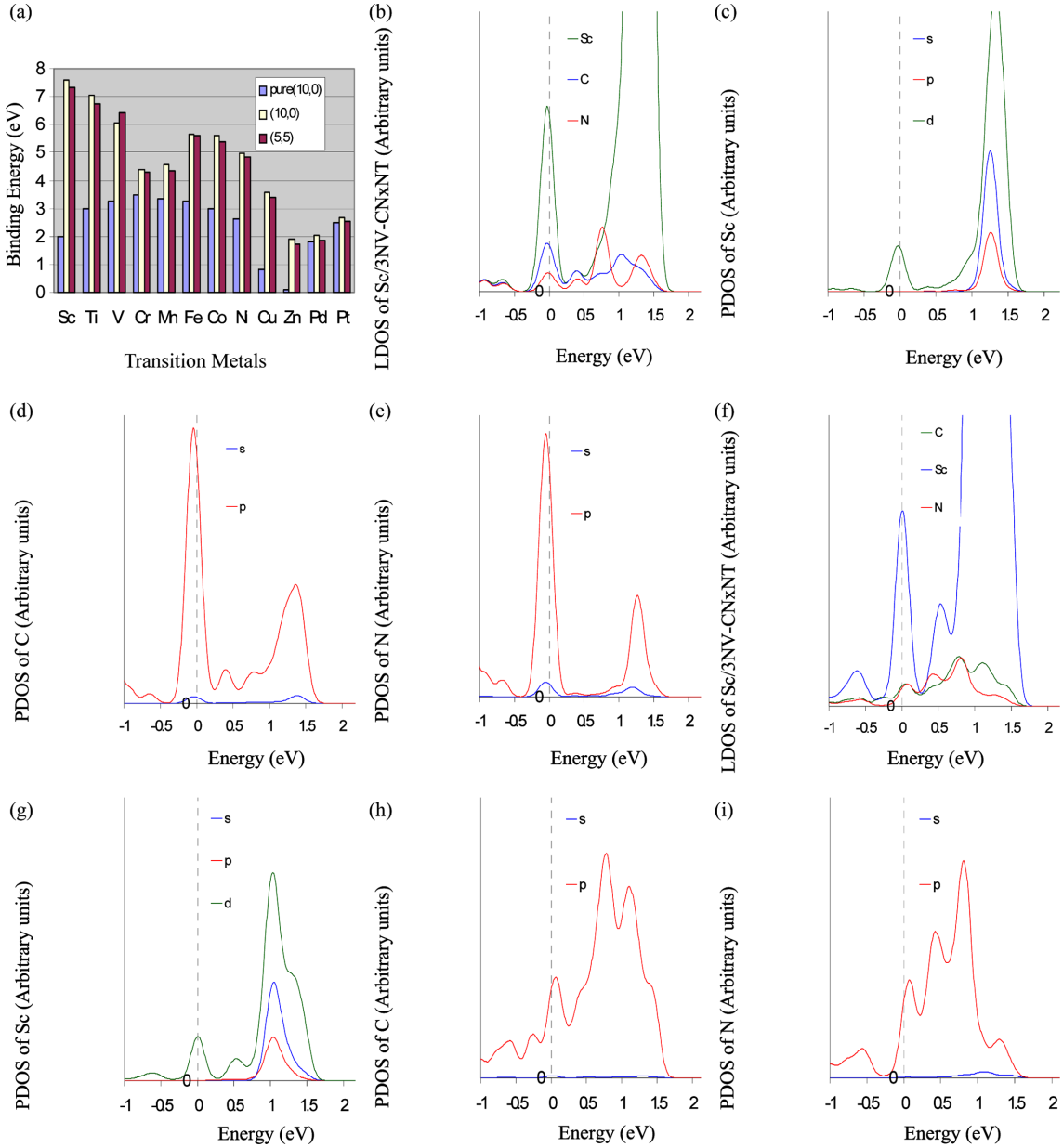

***Fig.* 4.** (a) The calculated binding energies (Eb) of the 12 different TMs on the pure CNT and CNT with pyridine-like defects, (b) The local densities of states (LDOS) of a Sc adsorbed on the (10,0) CNT with pyridine-like defects ($C_{116}N_3$), and the Partial densities of states (PDOS) of (c) Sc, (d) C, (e) N in the adsorption system for the (10,0) CNT. (f) The local densities of states (LDOS) of a Sc adsorbed on the (5,5) CNT with pyridine-like defects ($C_{96}N_3$), and the Partial densities of states (PDOS) of (g) Sc, (h) C, (i) N in the adsorption system for the (5,5) CNT.

Binding Energies

Two kinds of functionalized 3NV-CN_xNT with TMs were considered, as shown in *Fig*. 1d and 2d. The binding energy (E_b) of an individual TM on the 3NV-CN_xNT nanotube was defined as:

$$E_b = - E_{tot}(TM/3NV\text{-}CN_xNT) + E_{tot}(3NV\text{-}CN_xNT) + E_{tot}(TM) \quad (2)$$

where E_{tot} denotes the total energy of the optimized system in the bracket. Eb>0 corresponds a stable optimized configuration and indicates bonding.

On the other hand, due to the N participation and the vacancy defect, the binding energies of all TMs on the two 3NV-CN_xNTs are generally larger than those on the pure CNT[51,52] as shown in *Fig*. 4a. The formation of pyridine-like nitrogen defects is very crucial for enhancing the metal binding to the defects. Moreover, the variation of the binding energy as the number of d electrons for these TMs is also given in *Fig*. 4a we find that Sc ($3d^14s^2$), form the stronger bonds with E_b around 8 eV with respect to the others, which well agrees with previous study.[40] On the contrary, the binding energies of Zn ($3d^{10}4s^2$) on the two 3NV-CN_xNT are the smallest around 2 eV.

The strong interactions between these TMs and the two 3NV-CN_xNT nanotubes can be explained through the local densities of states (LDOS) and partial densities of states (PDOS), i.e., Sc adsorption on the 3NV-CN_xNT as shown in *Fig*. 4b-e for the (10,0) and *Fig*. 4f-i for the (5,0)

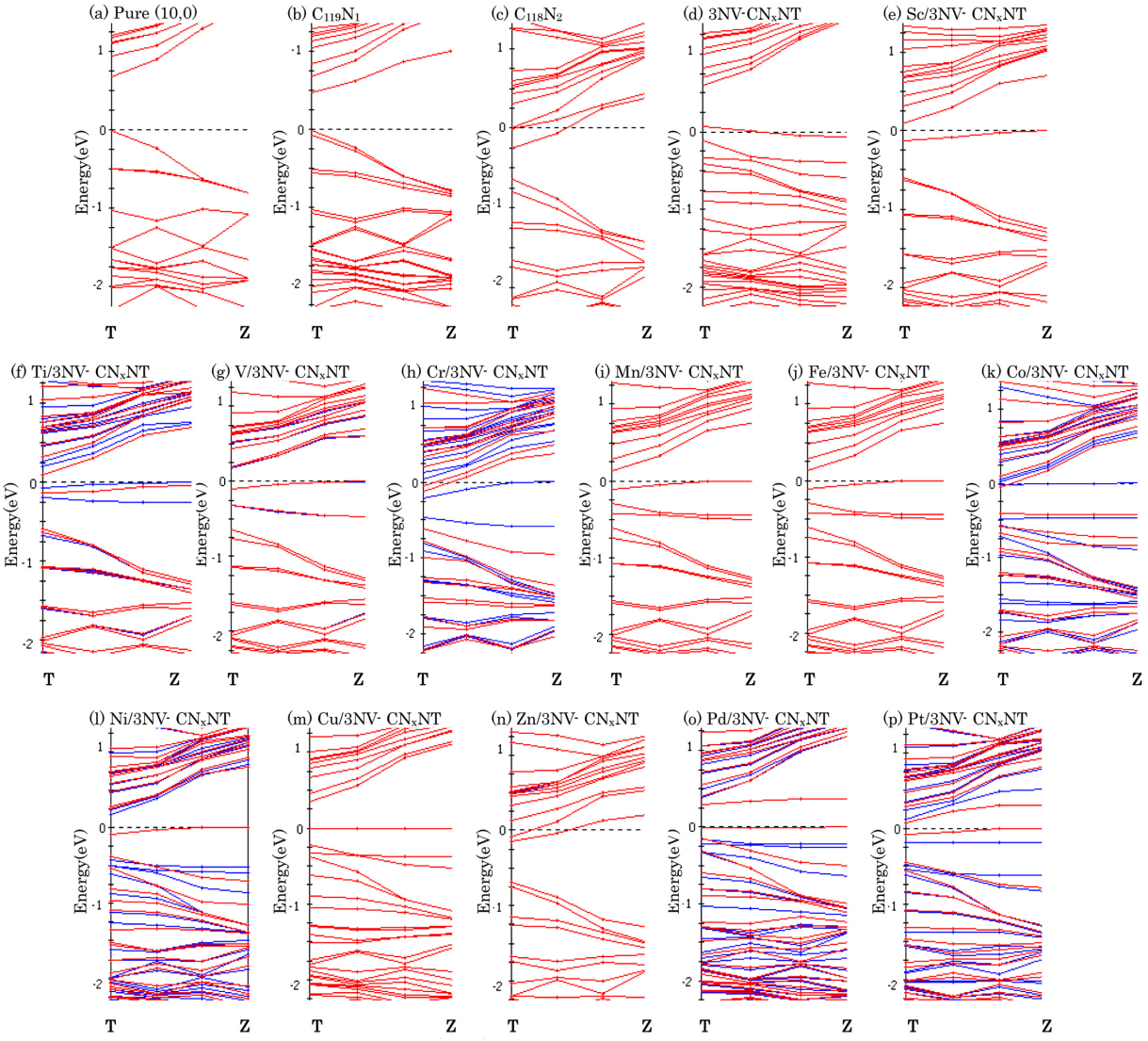

***Fig*. 5.** Band structures of TM-adsorbed on (10,0) zigzag CNxNT with 3NV defect. The Fermi level is set as zero and plotted with a dotted line. The blue and red plots denote alpha and beta band structures, respectively. Only one part indicates that this system is non-magnetic.

It is found that in both tubes the d electrons of Sc and the p electrons of C and N atoms mainly contribute to the electronic states near Fermi level. In other words, strong interaction exists between the d orbitals of Sc and the p orbitals of N atoms due to their hybridization with each other.

Electronic properties

Fig. 5a shows the band structure of a pure (10,0) nanotube, which is very similar to that in reference 54. The topmost valence band and bottom conduction band correspond to the big π-bonding and π*-antibonding states along the ring of the tube respectively. Upon nitrogenation, the degeneracies of the energy bands of (10,0) nanotubes are removed. That is, the presence of nitrogen impurities causes the band to split. Band structures of *Fig.* 5a-d are consistent with J. Zhao *et al*.[54] who have investigated the band structures of SWNTs with covalent sidewall functionalization (e.g. COOH, OH, F, H, CH3) and pointed out the marked difference between covalent functionalization and substitutional doping. As in the case of semiconducting (10,0) nanotubes, substitutional doping does not disturb the sp^2 hybridization of the π-electrons and the N impurity states contributes mainly to the minimum of the conduction band.

The electronic band structures of pure and doped (5,5) nanotubes are displayed in *Fig.* 6a-d. The π-π* band crossing of the pure (5,5) metallic tube is disturbed by the presence of N impurities. Small band gaps open up between

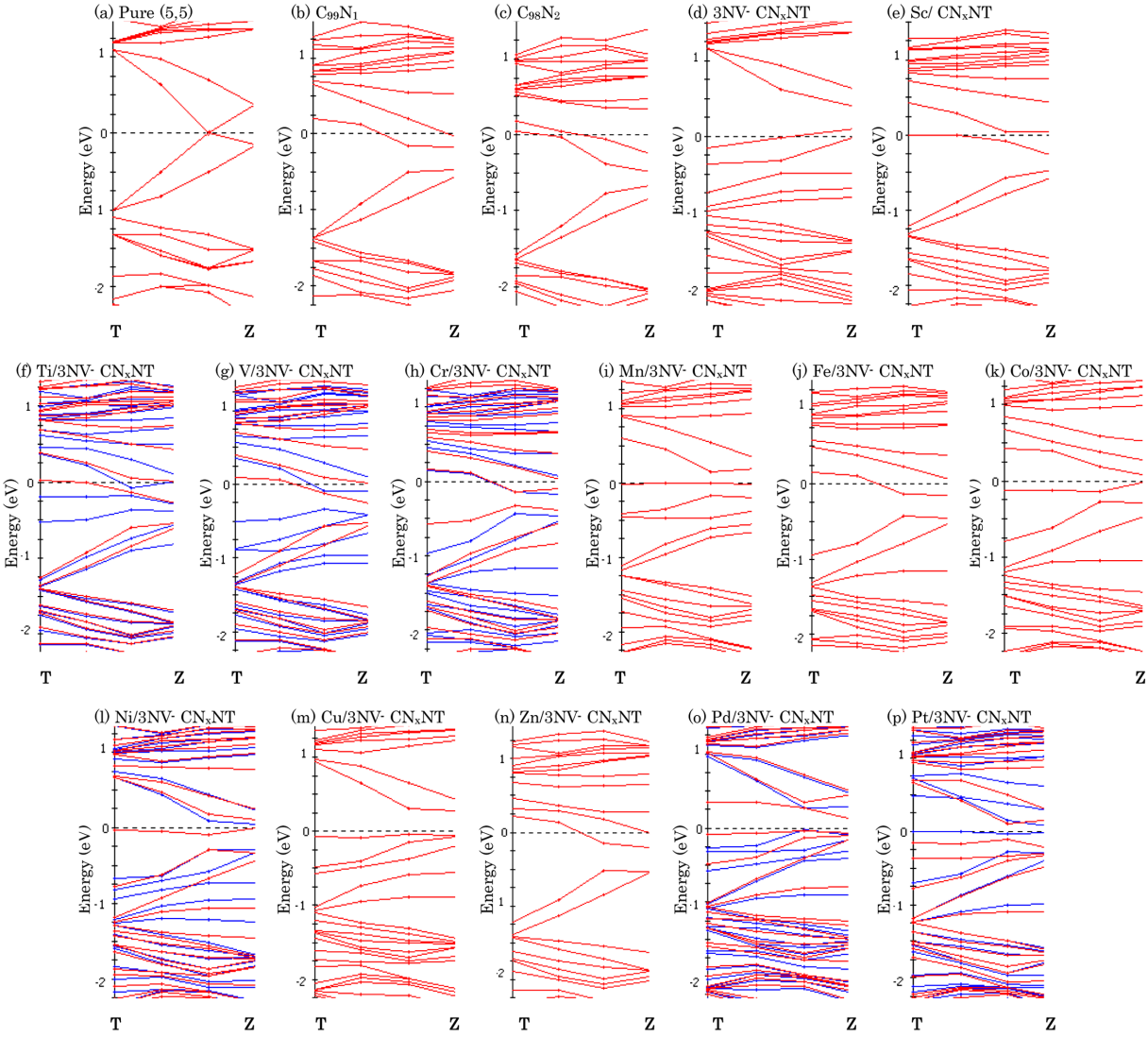

***Fig.* 6.** Band structures of TM-adsorbed on (5,5) armchair CNxNT with 3NV defect. The Fermi level is set as zero and plotted with a dotted line. The blue and red plots denote alpha and beta band structures, respectively. Only one part indicates that this system is non-magnetic.

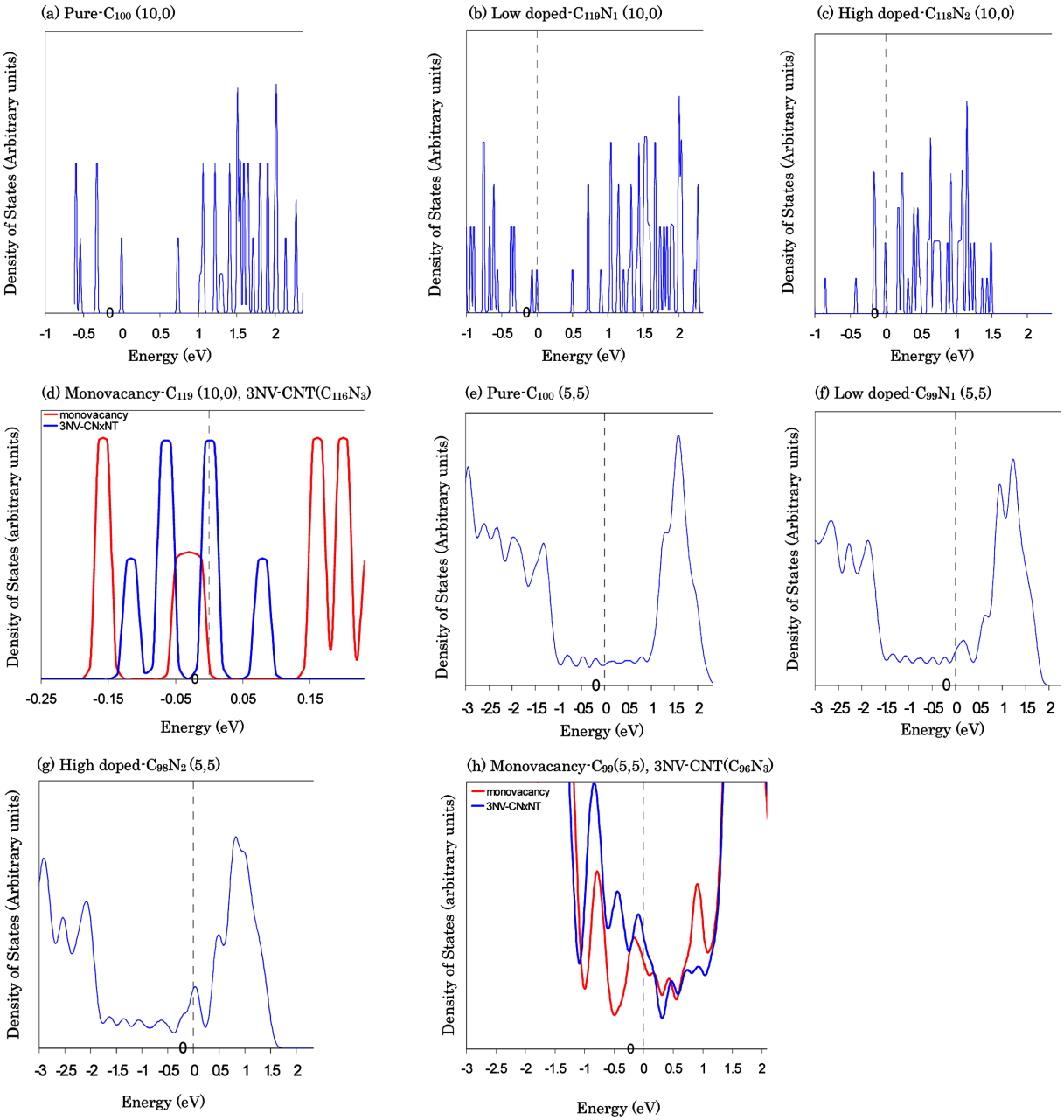

***Fig.* 7.** Total density of states (TDOS) of (a) pristine (10,0) nanotube, (b,c) nitrogen- substitution, (d) pyridine-like doping. Total density of states (TDOS) of (e) pristine (5,5) nanotube, (f,g) nitrogensubstitution, (h) pyridine-like doping. TDOS of undoped nanotube with monovacancy are indicated by red curves. The Fermi level is at 0eV and smearing of 0.0003 and 0.003 a.u. was applied for (10,0) and (5,5) graphs.

the conduction and valence bands, which are attributed to the breaking of the armchair nanotube mirror symmetry due to the tube-impurity interaction. The opening of small gaps has also been reported for covalently functionalized and Cu-adsorbed metallic nanotubes.[54,55]

In *Fig.* 7a-d, we present the electronic density of states (DOS) of pristine and nitrogenated (10,0) nanotubes. At low concentration of dopants (0.83%), direct substitution of nitrogen narrows the band gap. At higher level of doping, the band gap continues to narrow and eventually filled with impurity states at higher concentration of dopants. For instance, N-substituted (10,0) nanotubes of 1.67% become metallic due to the finite states at the Fermi level (see *Fig.* 7c). To investigate the effects of nitrogen impurities in the pyridine-like vacancy, we have also computed the DOS of a (10,0) tube with pyridine-like vacancy but

without nitrogen dopants (see the expanded view in *Fig.* 7d, red curve). The relaxed geometry of such a (10,0) tube with mono-vacancy without N-impurities shows that it is a semiconductor, while the (10,0) tube with pyridine-like nitrogen doping shows that it is a metal.

The electronic density of states of pure and nitrogenated armchair (5,5) nanotubes are displayed in Fig. 7e-h. The DOS of pure (5,5) tubes exhibit a finite DOS at the Fermi level, which renders it metallic. The presence of small valleys in the vicinity of the Fermi level is also observed for other nitrogenated (5,5) tubes, and this is mainly due to the broken mirror symmetry of the π-π^* band crossing. For the case of (5,5) tube with pyridine-like doping (*Fig.* 7h), a peak at the Fermi level is observed. Likewise, we have also computed the DOS of (5,5) tubes with pyridine-vacancy without N-impurities, and its DOS also shows a sharp peak at the Fermi level (see expanded view in *Fig*. 7h, red region). The DOS of pyridine-like nitrogenated (5,5) tubes is quite similar to (5,5) tubes with mono-vacancy (without N-impurities). Therefore the observed DOS peak at the Fermi level of the pyridine-like nitrogenated (5,5) tube is due the vacancy and not the nitrogen dopants.

Creation of new energy levels in the band gap with associated electronic states is an important step to make electronic devices thus we have carried out the chemical functionalization of nanotubes with the TMs. In *Figs*. 5e-p and 6e-p, we present the band structures of different TM/CN_xNT nanotubes. It can be seen that (10,0) and (5,5) CN_xNT with 3NV exhibits metallic nature (*Fig*. 5d and 6d), which are in good agreement with Li's study.[21] Upon adsorption of these TMs on the two CN_xNT, certain impurity states are introduced into their band structures, rendering that their electronic properties are changed to different degrees, which is strongly dependent on the adsorbed TMs. For example, Sc adsorption makes the two CN_xNT possess metallic nature, upon adsorption on their surfaces. Moreover, when Mn, Ni, Cu, Pd, or Pt is adsorbed on the two CN_xNTs, their band gaps are increased to different degrees due to the lift of the conduction bands of the two CN_xNTs. Thus, the several nanocomposites are still semiconductors.

Interestingly, three exceptions are Ti,V, and Co, adsorptions, for which the influences on electronic properties of the two CN_xNTs are completely different: (1) for the Ti adsorption, the (10,0) CN_xNT with 3NV defect is changed into a semiconductor while the (5,5) CN_xNT with 3NV defect has metallic nature; (2) when V adsorption, the 3NV-CN_xNT possess semiconductor nature (for(10,0)) and metallic (for(5,5)); (3) upon Co is adsorbed, the (10,0) CN_xNT with 3NV defect is transformed into a half-metallic material, while the (5,5) CN_xNT with 3NV defect is still a semiconductor and this gives one an inspiration: CN_xNT-based devices with various electronic properties can be achieved.

The changes in band structures of the CN_xNTs upon adsorption of these TMs are also evident by the charge transfer between the TM and the CN_xNT. As shown in *Table* 2, in which we list the calculated charge transfer using Hirshfeld population analysis[56], the charges transferred from TMs to the (10,0) CN_xNT with 3NV defect range from 0.70 e (for Sc) to 0.16 e (for Ni), while the range of charge transfer is from 0.70 e (for Sc) to 0.19 e (for Ni) in the case of (5,5) 3NV-CN_xNT. The charge transfer leads to the partially cationic of these TMs, and thus facilitating the adsorption of foreign species such as hydrogen gas, it follows that 3NV-CN_xNT doped with TMs is a potential material for hydrogen storage. On the other hand, we also evaluate the effects of TM adsorption on the magnetic properties of the two CN_xNT. We find that the net magnetic moment emerges, ranging from 1.85 (for Cr/3NV-CN_xNT) to 0 μ_B (for Sc/, Mn/, Fe/, Cu/, or Zn/3NV-CN_xNTs) for the (10,0) tube and from 2.54 (for V/3NV-CN_xNT) to 0 μ_B (for Sc/, Mn/, Fe/, Co/, Cu/, or Zn/3NV-CN_xNTs) for the (5,5) tube as shown in *Table* 2. This is reasonable, because the ground states of the two CN_xNTs are non-magnetic, and the net spin magnetic moment mainly originates from the contributions of TMs.

CONCLUSIONS

The structural, electronic and magnetic properties of the nitrogenation of (5,5) and (10,0) nanotube coupled with the chemical functionalization of nanotube with pyridine-like defect with 12 different TMs (Sc, Ti, V, Cr, Mn, Fe, Co, Ni, Cu, Zn, Pd, and Pt) are systemically studied, using first-principles methods investigated within the framework of the density functional theory using mainly the spin-polarized calculations. The effects of different types of nitrogenation have been elucidated from the band structures, density of states (DOS), and molecular orbital. Our calculations indicate that the substitutional nitrogenation, will convert semiconducting (10,0) nanotubes (~0.7 eV band gap) into metallic; while pyridine-like nitrogenation do not significantly modify the band gap. Also, electronic structures depend on the sites the nitrogen atoms occupy suggesting a way to control the electronic properties not only by adjusting the doping concentration but also the

doping sites can be realized. For metallic (5,5) nanotubes the N-doping is shown to significantly enhance the state density at the vicinity of Fermi level, which can enhance its chemical activity.

The effects of the chemical functionalization of TMs on the two 3NV-CN_xNT indicate that the electronic and magnetic properties can be effectively modified. These results show the interesting possibilities of tailoring the properties of nanotubes by TM doping. A metallic, half metallic, a semiconducting CN_xNT with different band gap can be achieved by chemical functionalization.

REFERENCES

1. Tasis, D.; Tagmatarchis, N.; Bianco, A.; Prato, M. *Chem. Rev.* **2006**, *106*, 1105.
2. Zhao, Y. L.; Stoddart, J. F. *Acc. Chem. Res.* **2009**, *42*, 1161.
3. Khabashesku, V. N.; Billups, W. E.; Margrave, J. L. *Acc. Chem. Res*. **2002**, *35*, 1087.
4. Niyogi, S.; Hamon, M. A.; Hu, H.; Zhao, B.; Bhowmik, P.; Sen, R.; Itkis, M. E.; Haddon, R. C. *Acc. Chem. Res*. **2002**, *35*, 1105.
5. Banerjee, S.; Hermraj-Benny, T.; Wong, S. S. *Adv. Mater.* **2005**, *17*, 17.
6. David, A. B.; Khlobystov, A. N. *Chem. Soc. Rev.* **2006**, *35*, 637.
7. Sen, R.; Satishkumar, B. C.; Govindaraj, A.; Harikumar, K. R.; Renganathan, M. K.; Rao, C. N. R. *J. Mater. Chem.* **1997**, *12*, 2335.
8. Terrones, M.; Terrones, H.; Grobert, N.; Hsu, W. K.; Zhu, Y. Q.; Hare, J. P.; Kroto, H. W.; Walton, D. R. M. Ph Kohler-Redlich, Rühle, M.; Zhang, J. P.; Cheetham, A. K. *Appl. Phys. Lett*. **1999**, *75*, 3932.
9. Czerw, R.; Terrones, M.; Charlier, J. C.; Blasé, X. B.; Foley, R.; Kamalakaran, N.; Grobert, H.; Terrones, D.; Tekleab, P. M.; Ajayan, W.; Blau, M.; Carroll, D. L. *Nano Lett*. **2001**, *1*, 457.
10. Terrones, M.; Ajayan, P. M.; Banhart, F.; Blase, X.; Carroll, D. L.; Charlier, J. C.; Czerw, R.; Foley, B.; Grobert, N.; Kohler-Redlich, Ph.; Rühle, M.; Seeger, T.; Terrones, H. *Appl. Phys. A: Mater. Sci. Process* **2002**, *74*, 355.
11. Golberg, D.; Dorozhkin, P. S.; Bando, Y.; Dong, Z. C.; Tang, C. C.; Uemura, Y.; Grobert, N.; Reyes-Reyes, M.; Terrones, H.; Terrones, M. *Appl. Phys. A: Mater. Sci. Process* **2003**, *76*, 499.
12. Villalpando-Páez, F.; Romero, A. H.; Mñoz-Sandoval, E.; Martínez, L. M.; Terrones, H.; Terrones, M. *Chem. Phys. Lett*. **2004**, *386*, 137.
13. Suenage, K.; Johansson, M. P.; Hellgren, N.; Broitman, E.; Wallenberg, L. R.; Colliex, C.; Sundgren, J.; Hultman, L. *Chem. Phys. Lett*. **1999**, *300*, 695.
14. Lim, S. H.; Elim, H. I.; Gao, X. Y.; Wee, A. T. S.; Ji, W.; Lee, J. Y.; Lin, J. *Phys. Rev. B* **2006**, *73*, 045402.
15. Droppa Jr., R.; Ribeiro, C. T. M.; Zanatta, A. R.; dos Santos, M. C.; Alvarez, F. *Phys. Rev. B* **2004**, *69*, 045405.
16. Villalpando-Paez, F.; Zamudio, A.; Elias, A. L.; Son, H.; Barros, E.; Chou, B. S. G.; Kim, Y. A.; Muramatsu, H.; Hayashi, T.; Kong, J.; Terrones, H.; Dresselhaus, G.; Endo, M.; Terrones, M.; Dresselhaus, M. S. *Chem. Phys. Lett.* **2006**, *424*, 345.
17. Yu, S. S.; Wen, Q. B.; Zheng, W. T.; Jiang, Q. *Nanotechnology* **2007**, *18*, 165702.
18. Qiao, L.; Zheng, W. T.; Xu, H.; Zhang, L.; Jiang, Q. *J. Chem. Phys*. **2007**, *126*, 164702.
19. Min, Y. S.; Bae, E. J.; Kim, U. J.; Lee, E. H.; Park, N. J.; Hwang, C. S.; Park, W. J. *Appl. Phys. Lett*. **2008**, *93*, 043113.
20. Rocha, A. R.; Rossi, M.; Fazzio, A.; da Silva, A. J. R. *Phys. Rev. Lett*. **2008**, *100*, 176803.
21. Li, Y. F.; Zhou, Z.; Wang, L. B. *J. Chem. Phys*. **2008**, *129*, 104703.
22. Gong, K. P.; Du, F.; Xia, Z. X.; Durstock, M.; Dai, L. M. *Science* **2009**, *323*, 760.
23. Ayala, P.; Arenal, R.; Rümmeli, M.; Rubio, A.; Pichler, T. *Carbon* **2010**, *48*, 575.
24. Yoon, H.; Ko, S.; Jang, J. *Chem. Commun.* **2007**, *14*, 1468.
25. Shao, Y.; Sui, J.; Yin, G.; Gao, Y. *Appl. Catal., B* **2008**, *78*, 89.
26. Su, F. B.; Tian, Z. Q.; Poh, C. K.; Wang, Z.; Lim, S. H.; Liu, Z. L.; Lin J. Y. *Chem. Mater*. **2010**, *27*, 832.
27. Li, X. G.; Park, S.; Popov, B. N. *J. Power Source* **2010**, *195*, 445.
28. Shao, Y. Y.; Liu, J.; Wang, Y.; Lin, Y. H. *J. Mater. Chem*. **2009**, *19*, 46.
29. Gregory, G.; Wildgoose, C.; Banks, E.; Richard, G. C. *Small* **2006**, *2*, 182.
30. Georgakilas, V.; Gournis, D.; Tzizios, V.; Pasquato, L.; Guldi, D. M.; Prato, M. *J. Mater. Chem*. **2007**, *17*, 2679.
31. White, R. J.; Luque, R.; Budairn, V. L.; Clark, J. H.; Macquarrie, D. J. *Chem. Soc. Rev*. **2009**, *38*, 481.
32. Yue, B.; Ma, Y. W.; Tao, H. S.; Yu, L. S.; Jian, G. Q.; Wang, X. Z.; Wang, X. S.; Lu, Y. N.; Hu, Z. *J. Mater. Chem.* **2008**, *18*, 1747.
33. Jiang, J. S.; Ma, Y. W.; Jian, G. Q.; Tao, H. S.; Wang, X. Z.; Fan, Y. N.; Lu, Y. N.; Hu, Z.; Chen, Y. *Adv. Mater.* **2009**, *21*, 4953.
34. Zhou, Y.; Pasquareli, R.; Holme, T.; Berry, J.; Ginley, D.; O'Hayre, D. R. *J. Mater. Chem*. **2009**, *19*, 7830.
35. Lepró, X.; Terrés, E.; Vega-Cantú, Y.; Rodríguez-Macías, F. J.; Muramatsu, H.; Kim, Y. A.; Hayahsi, T.; Endo, M.; Torres, M.; Terrones, M. *Chem. Phys. Lett.* **2008**, *463*, 124.
36. Chen, Z.; Higgins, D.; Tao, H. S.; Hsu, R. S.; Chen, Z. W. *J. Phys. Chem. C* **2009**, *113*, 21008.
37. Sadek, A. Z.; Zhang, C.; Hu, Z.; Partridge, J. G.; McCulloch, D. G.; Wlodarski, W.; Kalantar-zadeh, K. *J. Phys. Chem. C* **2010**, *114*, 238.

38. Yang, S. H.; Shin, W. H.; Lee, J. W.; Kim, H. S.; Kang, J. K.; Kim, Y. K. *Appl. Phys. Lett*. **2007**, *90*, 013103.
39. Li, Y. H.; Hung, T. H.; Chen, C. W. *Carbon* **2009**, *47*, 850.
40. Feng, H.; Ma, J.; Hu, Z. *J. Mater. Chem*. **2010**, *20*, 1702.
41. Titov, A. V.; Zapol, P.; Král, P.; Liu, D. J.; Iddir, H.; Baishya, K.; Curtiss, L. A. *J. Phys. Chem. C* **2009**, *113*, 21629.
42. An, W.; Turner, C. H. *J. Phys. Chem. C* **2009**, *113*, 7069.
43. Stoyanov, S.; Titov, A. V.; Krl, P. *Coord. Chem. Rev.* **2009**, ***253***, 2852.
44. Delley, B. *J. Chem. Phys*. **1990**, *92*, 508.
45. Perdew, J. P.; Burke, K.; Ernzerhof, M. *Phys. Rev. Lett*. **1996**, *77*, 3865.
46. Delley, B. *J. Quant. Chem*. **1998**, *69*, 423.
47. Monkhorst, H. J.; Pack, J. D. *Phys. Rev. B* **1976**, *13*, 5188.
48. Sun, C.; Wang, H.; Hayashi, M.; Chen, L.; Chen, K. *J. Am. Chem. Soc.* **2006**, *128*, 8368.
49. Choi, H. C.; Bae, S. Y.; Park, J.; Seo, K.; Kim, C.; Kim, B.; Song, H. J.; Shin, H. J. *Appl. Phys. Lett*. **2004**, *85*, 5742.
50. Terrones, M.; Kamalakaran, R.; Seeger, T.; Ruhle, M. *Chem. Commun*. **2000**, *23*, 2335.
51. Durgun, E.; Dag, S.; Bagci, V.; Gulseren, T.; Yildirim, C. S. *Phys. Rev. B* **2003**, *67*, 201401.
52. Durgun, E.; Dag, S.; Ciraci, S.; Gulseren, O. *J. Phys. Chem. B* **2004**, *108*, 575.
53. Pan, H.; Feng, Y. P.; Lin, J. Y. *Phys. Rev. B* **2004**, *70*, 245425.
54. Zhao, J.; Park, H.; Han, J.; Lu, J. P. *J. Phys. Chem. B* **2004**, *108*, 4227.
55. Kong, K.; Han, S.; Ihm, J. *Phys. Rev. B* **1999**, *60*, 6074.
56. Hirshfeld, F. L. *Theor. Chim. Acta* **1997**, *44*, 129.